Role of Solvent-Anion Charge Transfer in Oxidative Degradation of Battery Electrolytes from Quantum Chemical Calculations

Eric R. Fadel,[†,‡,¶] Francesco Faglioni,[§] Georgy Samsonidze,[‡] Nicola Molinari,[†,‡] Boris V. Merinov,[‖] William A. Goddard III,[‖] Jeffrey C. Grossman,[¶] Jonathan P. Mailoa,[‡] and Boris Kozinsky[*,†,‡]

†*John A. Paulson School of Engineering and Applied Sciences, Harvard University, Cambridge, MA 02138, USA*

‡*Robert Bosch LLC, Research and Technology Center, Cambridge, MA 02139, USA*

¶*Department of Materials Science and Engineering, Massachusetts Institute of Technology, Cambridge, MA 02139, USA*

§*Department of Chemical and Geological Sciences, University of Modena and Reggio Emilia, Via Campi 103, 41125 Modena, Italy*

‖*Materials and Process Simulation Center, California Institute of Technology, Pasadena, CA 91125, USA*

E-mail: bkoz@seas.harvard.edu

Abstract

Electrochemical stability windows of electrolytes largely determine the limitations of operating regimes and energy density of Li-ion batteries, but the controlling degradation mechanisms are difficult to characterize and remain poorly understood. We use

computational quantum chemistry to investigate the oxidative decomposition mechanisms that govern voltage stability of multi-component organic electrolytes. We find that electrolyte decomposition is a compound process involving both the solvent and the salt anion and requires explicit treatment of their coupling. Surprisingly, the ionization potential of the combined solvent-anion system is often significantly lower than that of the isolated solvent or the anion. This mutual weakening effect is explained by the formation of the oxidation-driven anion-solvent charge-transfer complex, which we study for 16 anion-solvent combinations. Our new understanding of the microscopic details of the oxidation mechanism allows to formulate a simple but accurate predictive model that explains experimentally observed trends in the onset voltages of electrochemical degradation of electrolytes at oxidative conditions near the cathode interface. The computational model opens opportunities for rapid rational design of stable electrolytes for high-energy batteries.

Lithium ion batteries have become the most widespread electrochemical storage technology due to their high energy density making them ideal in portable applications.[1] However, their implementation for applications requiring higher energy and power density such as car batteries remains a challenge.[2] The necessary energy density for usage in fully electric cars requires advances in cathodic and anodic materials in order to increase the operating voltage and capacity.[1,2] However, with an increase of the operating voltage, the commonly used organic electrolytes become unstable and new electrolyte materials are needed to increase safety and cycle life while possessing a lithium ion conductivity of at least $10^{-2}\,\mathrm{S\,cm^{-1}}$ at room temperature, normally regarded as the threshold for technological viability.[1] The study of the voltage window in which a given electrolyte material remains stable, as well as the pathways of degradation of the electrolyte outside of this window, is particularly important to the design of improved battery materials and systems.[3,4] The breakdown of electrolytes is a complex interface phenomenon that is difficult to characterize experimentally, and computational simulations can give valuable insights into the key microscopic mechanisms. Through computations, one can access energy barriers, reaction energies and intermediate structures,

which are almost impossible to obtain from experiments during complex battery operation conditions.[5]

While there are computational efforts trying to include electrolyte oxidation and reduction effects happening at the electrolyte-electrode interfaces,[6–8] progress is slow due to the computational complexity of such simulations, and a practical approach is to investigate the intrinsic stability of the bulk liquid electrolyte. Bulk electrolyte studies have the potential to be used as a first filter when screening for improved material designs since they provide an upper bound to the voltage stability of the entire system.[9–11] In this direction, the vast majority of reported works focus on the decomposition of a single species of the electrolyte, the solvent or the anion. Focusing on the bulk stability of a single species (with the possibility of adding a simple implicit solvation method) allows for simpler and faster calculations and enables high throughput screening of electrolytes.[10,12] Under this approximation, it is also feasible to study oxidation mechanisms at the surface of the electrode.[6,7] While many studies include solvation effects only implicitly, e.g. with a polarizable continuum model (PCM),[10,12] it has been shown in other contexts, e.g. ionic liquids, that explicitly taking into account the solvent is important for examining stability, and different studies attempt to take these effects into account.[13,14] In Li-ion battery electrolytes, computational studies looking at specific oxidation mechanisms have shown that studying isolated species does not fully capture the intricate interactions at play between solvents and anions, and instead the correct approach is to investigate systems comprising multiple and explicit solvents and anions [15–19]. Studies using this approach have highlighted interesting properties of the oxidation processes in these systems of multiple electrolytic species, and, most importantly, they have observed a weakening of the solvents in the presence of anions, or even other solvents.[5,15,20] This is shown in calculations of the adiabatic ionization potential (IP), Highest Occupied Molecular Orbital (HOMO) levels and molecular geometry changes.[15,20] The cause of the observed weakening of the solvent have been attributed to intermolecular reactions driven by oxidation, such as hydrogen or fluorine transfer, which lower the oxidation

stability.[16,17,21] Experimental studies do not unanimously observe this phenomenon: while some report dependence of the solvent oxidation[22–24] on the anion, others do not find such behavior.[25,26] Thus degradation mechanisms remain poorly understood because of the complexity of the many possible pathways, and the limitations and cost of current computational methods. Here we introduce a different way of understanding intrinsic bulk electrolyte stability, decoupling the initial onset of oxidation from the subsequent degradation pathways, and provide a simple quantitatively predictive description for the oxidative stability of the complete realistic electrolyte consisting of solvent and ions.

Building on the aforementioned premises, in this work we treat explicitly the oxidation of anion-solvent complexes, and analyze the atomistic and electronic structure details of the interaction between the component species.

To study the vertical IP of these anion-solvent complexes, it is necessary to carefully choose the computational approach that most faithfully treats the ionization of systems of multiple molecules. Various flavors of density functional theory (DFT) and quantum chemical methods have been used extensively for accurate predictions of IPs. Unfortunately, commonly used functionals, such as PBE[27] and B3LYP,[28] are susceptible to self-interaction errors and spurious charge delocalization,[29,30] resulting in non-physical charge distributions, and incorrect predictions of the dependence of the IP on the number of nearby solvent molecules. Since our goal is to investigate the explicit coupling between the anion and the solvent in an oxidation process, we compare different DFT and hybrid DFT functionals and adopt a functional able to capture the size effects in anion-solvent complexes as accurately as possible. We find the M06-HF[31–33] functional to be a suitable option, and note that functionals without 100% of Hartree-Fock (HF) exchange at long range yield unphysical oxidation descriptions and suffer from charge delocalization phenomena,[30] despite being commonly adopted in the literature.[10,34] We then provide new insights into the behavior of the IP of a combined solvent-anion system. The main findings of this work are that (1) the ioniza-

tion potential of the combined solvent-anion system can be significantly lower than the IP of either the isolated solvent or the isolated anion; (2) the effect is driven by electrostatic stabilization of the oxidized charge-transfer complex; (3) upon ionization the charge can be removed either from the solvent or the anion depending on the electrolyte chemistry. Using a simple charge transfer model previously formulated in the context of molecular crystals,[35] we are able to provide a simple and intuitive understanding of the oxidation of solvent-anion pair, and predict whether the anion or one of the solvents is fully oxidized when removing an electron from the total electrolyte system. We are also able to quantitatively estimate the overall ionization potential of the combined anion-solvent system. Importantly, we observe that the near-field electrostatic interaction between the anion and the solvent plays a crucial role in the total electrolyte oxidation, due to the possibility of formation of the charge transfer complex. If the charge-transfer complex formation is energetically favorable, the overall IP is reduced relative to the IP of the solvent, which is often used as a proxy for electrolyte stability. This new interpretation not only accounts for the weakening effect of the solvent by the anion mentioned previously, but also explains the non-trivial correlation previously observed between the overall oxidation potential and the solvent HOMO level.[15,20]

This article is organized as follows. First, we present our study on the behavior of different semilocal functionals and hybrid functionals for the oxidation of multiple solvents or anions, and then for combined systems of an anion and solvents. Then we study the oxidation of combinations of four anions: 4,5-dicyano-2-(trifluoromethyl)imidazolium (TDI^-), bis-(trifluoromethane solfonimmide) ($TFSI^-$), tetrafluroborate (BF_4^-), hexafluorophosphate (PF_6^-), with four solvents: dimethyl sulfoxide (DMSO), dimethyl ether (DME), propylene carbonate (PC), acetonitrile (ACN). Our approach combines the use of classical molecular dynamics (MD) to obtain the representative structures of anion-solvent configurations and hybrid DFT to compute vertical IP for these structures. Finally, we present the main features of the simple charge transfer model we use to describe the oxidation of anion-solvent

complexes and verify its predictability against the computed IP data.

Methods

Throughout this work, the vertical ionization potential (IP) is computed using the ΔSCF formalism[10,14,34], hereafter denoted with $IP_{\Delta SCF}$. The vibrational contribution to the energy is neglected, as it is commonly found to account for a small correction to the IP.[12,17,36,37] All the reported partial charges are estimated using the Mulliken charge scheme,[38] and summed over every molecule (we omit diffusive orbitals in the basis set for the Mulliken charges calculations so as to avoid contamination of partial charges from adjacent atoms). The study of the effect of delocalization errors in different DFT functionals for systems of multiple $TFSI^-$ anions and/or DME solvents is performed using the Gaussian09 software,[39] with the 6-311++G**[40,41] basis set on all atoms. For each computational method considered, we perform geometry optimization followed by spin-unrestricted computation of the vertical IP.

In the second part of this study, we look at anions solvated by a different number of solvent molecules. Previous works have shown the importance of sampling electrolyte configurations,[13,18,34,36] and have done so using classical MD[34,36] or ab-initio MD.[13] In this work, the structures are obtained from snapshots of classical MD simulations, obtained as follows.

First, the anion of interest and the solvent molecules are placed on the vertices of a three-dimensional cubic grid, with the aim to create a low-density non-overlapping initial structure. Once generated, the structures are brought close to equilibrium by a series of energy minimization, compression/decompression, and annealing stages, broadly based on previous works,[42,43] to overcome local energy barriers in search of lower energy minima, and, ultimately, more representative structures. The structures are then evolved using the velocity-Verlet algorithm, with a time step of 1.0 fs, in the constant number of atoms, pressure, and temperature (or NPT) ensemble. Temperature and pressure are kept at 300 K and 1

atmosphere, respectively, with a Nosé-Hoover barostat and thermostat.[44–46] The coordinates of all atoms are saved every 10^3 timesteps (i.e., 1 ps) to ensure sufficiently uncorrelated structures. In post processing the positions of the anion and of the closest X solvent molecules (X ranging from one to five) are extracted from the snapshots and used in the ab-initio calculations. The structures do not undergo any further geometry optimization, instead we sample different configurations of this system in order to gather statistics on the IP of anion and solvent complexes. All molecular dynamics simulations are performed in the LAMMPS simulation package.[47] The interactions are modeled using the OPLS2005 force-field[48] from Schrodinger Inc. Since the MD structures do not undergo further geometry optimization, it is important to ensure that the configurations are well sampled by the classical energy model approximation. To this end, we consider a set of 200 configurations of the ($TFSI^-$, PC) pair and plot in Figure 1(a) the energy for these configurations computed with the classical force-field (red) and with DFT (blue). The two distributions are Gaussian-like, with the classical force-field underestimating the energy of the configurations compared to DFT, but preserving the distribution of the energy in the phase space. Thus we conclude that the OPLS2005 force-field samples configurations with reasonable accuracy. Figure 1(b) shows an example of a snapshot for the solvated anion (for clarity, not all solvent molecules are shown), in the case of the ($TFSI^-$, DME) pair, and Figure 1(c) to (e) examples of extracted configurations with one anion and its closest solvent for the same pair.

Ab-initio calculations were performed using the M06-HF hybrid functional with the NWCHEM software,[49] and for each pair we computed the IP of 30 different configurations obtained from the MD run. All calculations were spin-unrestricted, and the spin contamination of the system was consistently checked. The basis set used for all atoms was aug-cc-PVTZ.[50] No implicit solvation model was used for this part of the work, because we wish to study the IP of explicitly solvated anions with a functional that does not induce erroneous charge delocalization. The effect of implicit solvation and the limit of full solvation are also studied, and reported in the last section of this work. Finally, coupled-cluster with single, double,

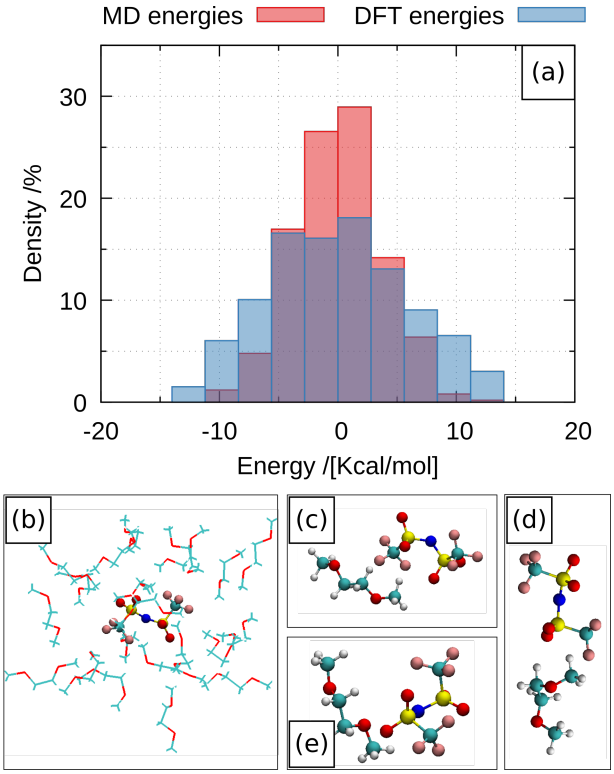

Figure 1: Figure (a) represents for 200 configurations of anion-solvent pairs from MD snapshots for the ($TFSI^-$, PC) pair, the distribution in energy computed from MD and the distribution of energy computed from DFT (M06-HF). Both these distributions are plotted relative to their average. (b) shows a solvated anion for an MD snapshot in the case of the ($TFSI^-$, DME) pair. (c) to (e) show examples of configurations of solvent-anion pair from MD snapshots for the ($TFSI^-$, DME) pair.

and perturbative triple excitations (CCSD(T)) calculations were performed to validate our approach. These calculations were performed using ORCA,[51] in the Domain-Based Local Pair-Natural Orbital Coupled Cluster (DLPNO-CCSD(T)) approximation. The basis set for these calculations was aug-cc-PVDZ.[50] For reference, we also compute the IP of the isolated species (anion or solvent in vacuum). The IP shown for the isolated species is the average IP from 50 different configurations taken from MD (created with a single molecule in a cubic box with 100 Å side and using the same force field).

Results and Discussion

Study of Charge Delocalization and Self Interaction Correction

In this section we point out the importance of managing the spurious charge delocalization issues present in semi-local DFT calculations of oxidized molecular systems consisting of multiple components. The key results are summarized in Table 1, which shows IPs and charge study for different functionals and different configurations. Gas phase anion and solvent IPs are reported in column two and three. In columns 4-9 and 10-15, results are presented for systems of five identical anions 500 Å apart and five identical solvents 10 Å apart, in vacuum. The last five columns present configurations of one $TFSI^-$ molecule solvated by three DME molecules. Structures obtained from optimizing the geometry with the different ab-initio methods are slightly different, but qualitatively the same. We find that only methods including 100% long range HF exchange (LC-BLYP, M06-HF, and HF) correctly describe the removal of the electron from a single molecule in the cases of 5 anions or 5 solvents. In these cases, the IP is almost independent of the number of molecules in the

Table 1: Ionization Potential (eV), and charge distribution for different systems computed in vacuum with different functionals. For reference, in the case of DME, the experimental IP is 9.8 eV and our calculated DLPNO-CCSD(T) IP is 9.9 eV. For $TFSI^-$ our calculated DLPNO-CCSD(T) IP is 7.3 eV. These values are reported in table S8 in the supplementary information. Columns 2 and 3 refer to isolated DME and $TFSI^-$, respectively. Columns 4-9: five identical DMEs 10 Å apart. Columns 10-15: five identical $TFSI^-$ molecules 500 Å apart. Columns 16-21: one $TFSI^-$ solvated by three DMEs. The fraction of an electron removed from each anion (A) or solvent (S) molecule is proportional to the intensity of blue in the corresponding column.

Method	DME	$TFSI^-$	DME_5						$TFSI^-{}_5$						$TFSI^-$+DME_3				
			IP	S	S	S	S	S	IP	A	A	A	A	A	IP	A	S	S	S
PBE	8.75	5.82	6.77						3.60						4.99				
PBE0	9.34	6.86	8.06						4.85						6.07				
B3LYP	9.30	6.85	7.88						4.70						5.91				
B3LYP-D3	9.30	6.85	7.88						4.71						5.80				
M06-2X	9.92	7.26	9.36						6.22						6.85				
CAM-B3LYP	9.73	6.72	9.16						6.08						6.86				
LC-BLYP	10.13	7.17	10.11						7.08						7.23				
M06-HF	10.24	7.93	10.20						7.66						7.27				
HF	8.82	6.30	8.80						6.17						6.45				

calculation, as physically expected. Similarly, in the case of one $TFSI^-$ anion surrounded by DME solvents, only LC-BLYP,[52,53] M06-HF, and HF correctly remove an electron from a single molecule, namely one of the DMEs. All other functionals, including some commonly used semi-local functionals, nonphysically delocalize the charge, removing a fraction of an electron from all molecules. More results for this study are presented in the supplementary information, with PF_6^- as the anion (see table S5), or showing that the results persist when adding implicit solvation (table S4). Finally, we note that in the case of $TFSI^-$ and three DME, the functionals that completely oxidize one molecule oxidize the solvent, which has a higher IP than the anion. This is counter-intuitive, and we discuss in detail in the rest of this work how charge-transfer pair formation is the cause of this oxidation mechanism. The phenomenon of charge-transfer upon oxidation of the anion-solvent complex, i.e. removal of the electron from the molecule with higher IP, is the focus of the next sections. As mentioned in the introduction, this effect was described in previous works as a consequence of reaction that follows oxidation, but here we emphasize that it occurs already in the calculations of the vertical IP, independent of chemical degradation pathways.

In summary, only functionals with 100 % of HF exchange at long range (HF, M06-HF, LC-BLYP) yield the correct ionization behaviors and do not suffer from charge delocalization, while methods without full HF exchange misrepresent the oxidized state, predicting charges delocalized on more than one molecule. We also mention that recent work on ionic liquids showed that range-separated functionals suffer much less from self-interaction delocalization error and show similar dipole moments and interaction energies as wave-function methods.[30] From our study of charge delocalization in DFT functionals, M06-HF is inferred to be an appropriate functional to study the effect of explicit solvation on ionization in a wider set of chemistries and geometries. However we also observe that the isolated IP from M06-HF for the molecules, whether solvents or anions, are found to be overestimates of the experimental values. The inaccuracy of M06-HF is a known problem, and it persists when computing IP from optimized geometries. In this work, emphasis is placed on the

correct treatment of ionization and minimizing delocalization error, focusing on the physical mechanism of ionization and the origins of charge transfer in solvent-anion complexes. Most trends presented here are significant in comparison with the IP errors and are fundamentally not altered by the inaccuracies arising from the functional. Here we also note that none of these functionals is as accurate as CCSD(T) for IP. However, their lower computational cost allows us to study systems of multiple molecules otherwise practically impossible with CCSD(T) level of theory.From the results of our DLPNO-CCSD(T) calculations reported in the supplementary information (table S8), we find that it is possible to get very accurate IP values (compared to experimental measurements) with a more accurate method when required. Furthermore, we find that M06-HF accuracy is satisfying for the chemistries studied in this work, with an error smaller than the spread of the IP over different configurations. Furthermore, we discuss later in this paper that although the absolute values of the IP for the different systems may be different between methods, the trends and phenomena described in this work remain valid even when analyzing DLPNO-CCSD(T) results.

IP values of anion-solvent pairs

In this section, we present the results for the IP study of anion-solvent pairs, and provide a simple empirical formula for the IP of the pair, before proposing a simple physical model in the next section. First, we find that the spread of the IP values over all the snapshot configurations is significant (on the order of 1 eV), across all chemistries.

To investigate this spread we study two specific couples, ($TFSI^-$, PC) and (PF_6^- , DME), using 200 configurations of the anion-solvent pair. Figure 2 shows the obtained distributions of vertical IP. The first pair comprises $TFSI^-$ that is a "weak" anion (i.e., has an IP in gas phase of 7.23 eV), and PC that is a "strong" solvent (i.e., has an IP of 12.66 eV). The second pair comprises a "strong" anion (PF_6^- with an average IP of 9.7 eV), and a "weak" solvent (DME with an average IP of 10.2 eV). We indeed find that the spread is significant, but that the average distribution converges for a moderate number of configurations (for ($TFSI^-$,

PC) for example, the average with 30 random configurations is 7.5 eV and the average with 200 random configurations is 7.45 eV). The use of 30 random configurations is deemed a good compromise between computational cost and accuracy, and therefore applied to the study of all anion-solvent pairs.

We also plot the heat maps of the initial and final energies with respect to the ionization potential (Figure 2) for these two anion-solvent pairs. We find that there is a distinction between anion-solvent pairs for which the anion is oxidized, and those for which the solvent is oxidized. For the ($TFSI^-$, PC) pair, the anion is the species that is oxidized. In this case, for configurations with IP near the average the IP peak, the configuration's initial and final energies are near the average of their respective distributions. For configurations corresponding to the lower end of the IP distribution, their initial energy is high relative to the set of all configurations and their final energy is low. Inversely, configurations with high IP have low to average initial energy but high final energies. Considering the (PF_6^- , DME) pair in which the solvent is oxidized, we find a very different behavior: the initial energy is relatively uncorrelated to the IP of the configuration, and the distribution of IP is mostly governed by the final energy. This difference is significant and highlights a difference in the oxidation mechanism which can be understood using the model discussed later in this work.

Because of this spread, we conclude that sampling many different configurations is essential to properly describe oxidation of realistic solutions at finite temperature. We also note that in principle the stability of the system could be inferred from the IP distribution across different solvation structure configurations. Neglecting interface reactions and considering only intrinsic oxidation stability, one can suppose that the onset of electrolytes' degradation is determined by the lower edge of the distribution of IP values. Indeed, assuming that electron transfer during oxidation occurs much faster than the nuclear dynamics of the system, and given that many different configurations will be explored over time in the vicinity of the electrode, those configurations that are more easily oxidized will limit the stability of the

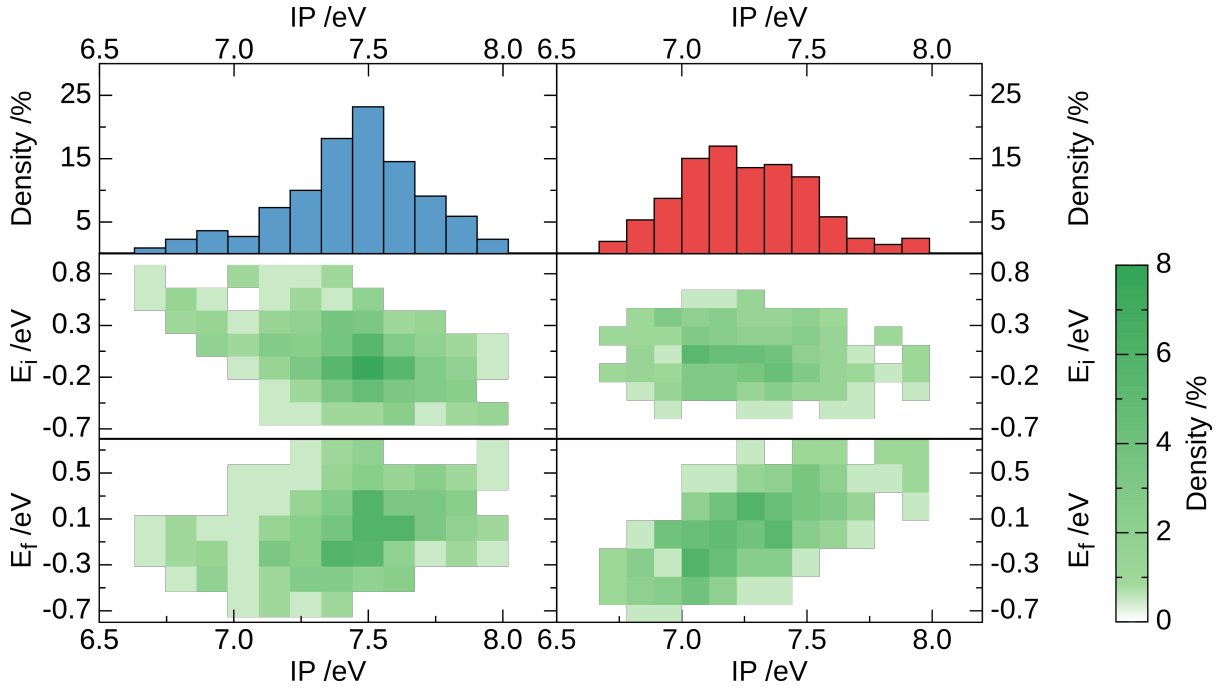

Figure 2: IP distribution for 200 random configurations of anion-solvent pair. The first column corresponds to the ($TFSI^-$, PC) pair, and the second column corresponds to the (PF_6^- , DME) pair. Supplementary information reports a full study for all anion-solvent pairs (figure S3) with 30 configurations. The color code, which is consistent in all this work, represents in blue configurations where the anion is fully oxidized (as is the case for all configurations of the ($TFSI^-$, PC) pair) and in red configurations where the solvent is oxidized (as is the case for all configurations of the (PF_6^- , DME) pair). Below these two figures, we plot the heat maps of the initial (middle plot) and final (bottom plot) energies for the two pairs. The energies are plotted relative to the average energy (either initial or final).

electrolyte. The whole IP distribution allows to understand the stability of the electrolyte as the voltage is increased past this threshold value. Indeed, in cyclic and differential voltammetry experiments the measured electrical current due to degradation exhibits gradual increase with electrode voltage, qualitatively consistent with our computational result. For all the chemistries we studied, the IP distribution has a single peak and is centered at its average (see supplementary information figure S3). Interestingly, the spread of the distribution was not found to depend significantly on chemistry, but does depend on which species (the anion or the solvent) is oxidized during overall oxidation (this is discussed in detail below and in the supplementary information). In the rest of the study, we therefore focus on IP

trends inferred from the average IP across several configurations as these averages accurately represent the IP distributions.

The average IP of 30 configurations for each anion-solvent pair are reported in Figure 3. The IP values of the anion-solvent exhibit a non trivial relationship to the IP values of each

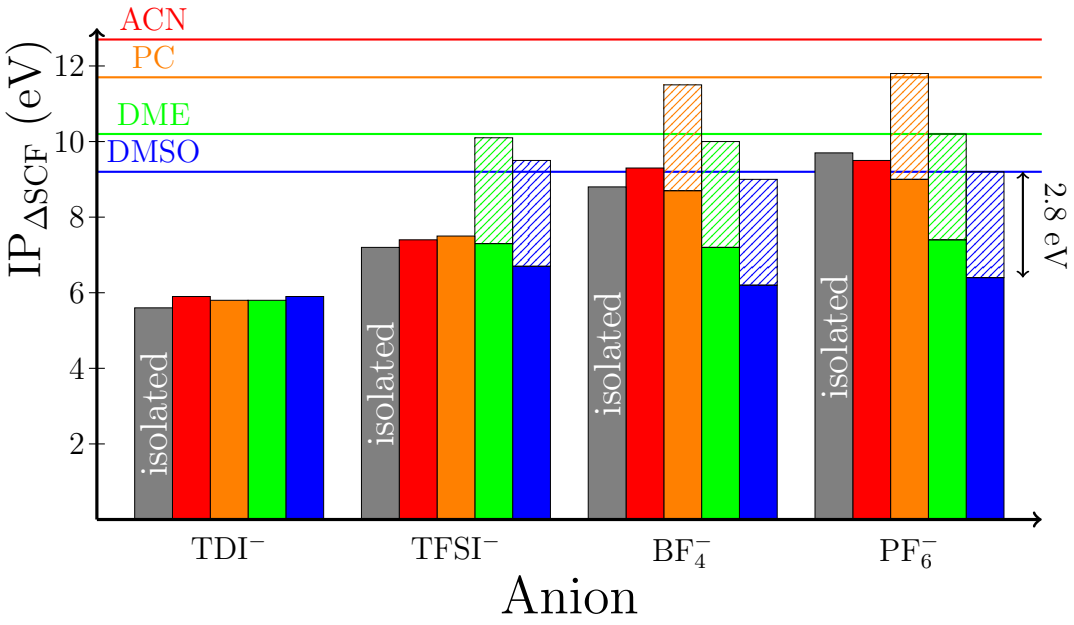

Figure 3: IP of pairs of one anion and one solvent molecule with respect to the isolated species. Bars represent the average over 30 configurations of each pair, with the x-axis showing the anion and the color indicating the solvent used (blue: DMSO; green: DME; orange: PC; red: ACN; grey: isolated anion). Values for the isolated species (y-axis for the solvent, grey bar for the anion) are averaged over 50 configurations. Dashed bars represent constant shifts δ =2.8 eV (drawn for pairs where the solvent is oxidized). IPs are well approximated by Equation 1: the smaller of anion IP or the solvent IP minus δ.

individual component. Contrary to common assumptions, the overall IP is not determined by that of the solvent alone, as shown by the lack of solvent dependence in the IP of combinations containing TDI^- (weakest anion). On the other hand, the solvent has a clear effect on the IP of combinations containing PF_6^- (strongest anion). Importantly, in no case is the overall IP equal to that of the solvent. We now examine this trend quantitatively and later will provide a physical explanation. This overall trend is captured quite well by Equation 1, where A^- is the anion, S the solvent, $[AS]^-$ is the pair of anion and solvent before oxidation and $\delta = 2.8$ eV:

$$IP_{\text{fit}}\left([AS]^{-}\right) = \min \begin{cases} IP\left(A^{-}\right) \\ IP\left(S\right) - \delta \end{cases} \tag{1}$$

When the IP of the isolated anion is smaller than that of the solvent by more than δ, for example in the case of pairs (TDI^- , DMSO), (TDI^- , DME), or ($TFSI^-$, ACN), the combined system IP is roughly that of the anion, and the charge study shows that the electron is removed from the anion. On the other hand, when the IP of the isolated anion is greater than the IP of the solvent minus δ, for example for the pairs (BF_4^- , DMSO), (BF_4^- , DME), or (PF_6^- , PC), then the combined system is weaker than either species, and the IP of the pair is approximately equal to the IP of the isolated solvent minus δ. Our charge study in this case shows that the solvent is oxidized, which is contrary to common intuition, given that the solvent always has higher IP than the anion. This is highlighted in the graph using striped bars of height δ showing the difference between the isolated solvent IP and that of the anion-solvent pair. This behavior corresponds to switching from oxidizing the anion to oxidizing the solvent, in which case the IP becomes independent from the anion and equal to the solvent IP minus δ. This indicates that for many solvent-anion combinations a charge-transfer complex spontaneously forms upon oxidation, depending on the IP of individual species, with an electrostatic stabilization δ. We note that our combined simulations properly oxidize one molecule only (whether the anion or the solvent) in over 90% for all cases, further validating our choice of the exchange-correlation functional. Naturally, in borderline cases where the values in Equation 1 are similar, oxidation of either the anion or the solvent may be observed, depending on the specific geometry. In the rest of this article, we refer to the IP computed using Equation 1 as IP_{fit}.

We examined this effect using more accurate DLPNO-CCSD(T) calculations for the (TDI^- , PC), ($TFSI^-$, PC), (BF_4^- , PC) and (PF_6^- , PC) combinations, and the full results are reported in the supplementary information (tables S8 and S9). Briefly, we find not only that using a highly accurate level of theory yields IP values that closely agree with experi-

mental data, but also that the trends presented in this work remain unaltered (see table S9). This validates our computational approach with regards to the choice of the DFT functional.

Interpretation of previous experiments and computations

For further supporting evidence to our hypothesis, we compare our results with previous experimental and computational works from the literature. Comparison between computed IP and experimental IP as measured in gas phase is provided in the supplementary information. Focusing on the trends of oxidation voltage with respect to the choice of anion-solvent chemistry, we argue that the observed behavior will depend on which species is oxidized. When considering electrolytes with the same solvent species and varying anion species, the oxidation voltage will increase with increasingly "strong" anion (while the species that is oxidized is the anion, i.e. it is "weak" compared to the solvent), until it saturates when switching happens and the solvent becomes the oxidized species. Therefore we expect a dependence of the oxidation voltage on the anion, but only for anions that are "weak" enough. When keeping the same anion and changing the solvent species, two different effects are at play to determine the oxidation voltage: the oxidation mechanism (whether the anion or the solvent is oxidized) and the solvation effect, which leads to a more ambiguous, chemistry-dependent trend. Looking at the experimental observations by Ue *et al.*,[23,54] they first find that for a given solvent, (PC), the combined system oxidation potential depends on the anion IP, but that this dependence saturates for anions such as BF_4^- or stronger. Indeed, in their experimental results, the oxidation voltage for BF_4^- , PF_6^- and AsF_6^- are roughly the same, which in our understanding of oxidation, hints at a switching from anion oxidation to solvent oxidation. Then, they use a more oxidation-resistant solvent, glutaronitrile, in order to determine the anodic stability order of those anions. Thus, we find a situation where both anion and solvent oxidation matter, depending on which species is oxidized, and their study shows the two possible behaviors of oxidation voltage with changing anion. All these

observations are consistent and can be explained with our new understanding of oxidation. However, direct comparison to oxidation voltages as obtained through cyclic voltammetry measurements is not a well defined validation procedure for computational methods. These measurements have a large variance since they are affected by a wide range of parameters such as the scanning rate,[23] the nature of the electrode, the concentration of species in the electrolyte, and even the method adopted to infer the oxidation voltage from the raw data.[55] On the other hand, computational method suffer from DFT functional and basis set inaccuracies and approximate full solvation effects. In this work, emphasis was given to accurately describe oxidation mechanisms from the microscopic, ab-initio standpoint, compromising on the accuracy on the absolute value of the IP (also, surface effects are not taken into account). Furthermore, we did not take into account zero-point energies and vibrationnal entropy. Whilst, for these reasons, quantitative comparison with experimental results is difficult, we believe that the trends presented in this work give important insights into the possible oxidation scenarios.

Previous computational work by Kim et al[20] presented, without explanation, the location of the HOMO for different anion-solvent pairs, finding that the HOMO of the pair can be on the anion or on the solvent. Even though the exchange-correlation functional used (M06-2X) still has a degree of spurious delocalization (Table 1), the trend in the reported data is consistent with our hypothesis. The HOMO is always on the anion for a very weak anion (bis(oxalate)borate) across all studied solvents. However for a strong anion (PF_6^-), the HOMO is always on the solvent across all studied solvents. In intermediate cases such as for $TFSI^-$, the HOMO is on the solvent for the weaker solvents, but is on the anion for stronger solvents. The decrease of the overall IP of the anion-solvent combination relative to the IP of each species is explained in that work, and earlier ones,[15,56] as a consequence of intermolecular chemical reactions. Thus, we see strong evidence emerging that the oxidation of the electrolyte is controlled by *both* the anion and the solvent. However, in contrast to previous interpretations, we conclude that the weakening effect is driven by the spontaneous

charge-transfer between the anion and the solvent and does not require consideration of the specific reaction pathway following oxidation.

Charge transfer stability model

To understand the full chemistry dependence of electrolyte stability in terms of the solvent-anion charge transfer complex formation we derive a simple stability model, similar to the one used in the field of charge transfer in molecular crystals.[35] For a pair of molecules of anion A^- and solvent S, we can express the energy of the oxidized pair as:

$$E\left([AS]^0\right) = \min \begin{cases} E\left(A^0 S^0\right) \\ E\left(A^- S^+\right) \end{cases} \tag{2}$$

Therefore there is a trade-off between oxidizing the anion which is weaker or oxidizing the solvent and creating a dipole which lowers the electrostatic energy. This formula accounts for the trend presented in the previous section: when the anion is significantly weaker, the first expression is the minimum, i.e. the electrostatic gain is not sufficient for the solvent be oxidized. In cases where the anion IP is not significantly lower than the solvent IP, it will be more energetically favorable to form an electrostatic dipole by oxidizing the solvent. The threshold between the two cases is determined by the electrostatic energy δ of the dipole formed by oxidizing the solvent, as well as the individual IPs.

By considering the total energy of the system as a sum of the short-range quantum contribution (ionization) and a long-range electrostatic contribution (dipole energy), it is possible to derive from Equation 2 an expression for the pair IP. Denoting the classical electrostatic energy $E_e\left(X\right)$ for the molecular system X considered in isolation, and $E^{\text{bind}}\left(XY\right) = E_e\left(XY\right) - E_e\left(X\right) - E_e\left(Y\right)$, we have:

$$IP_{\text{model}}\left([A^{-}S^{0}]\right) = \min \begin{cases} IP\left(A^{-}\right) + E^{\text{bind}}\left([A^{0}S^{0}]\right) - E^{\text{bind}}\left([A^{-}S^{0}]\right) \\ IP\left(S^{0}\right) + E^{\text{bind}}\left([A^{-}S^{+}]\right) - E^{\text{bind}}\left([A^{-}S^{0}]\right) \end{cases} \tag{3}$$

The only approximation used to derive this expression is that the quantum (non-electrostatic) contribution to the total energy of a solvent-anion pair is short-ranged and is close to the sum of each component's quantum energy contribution. At the same time, the long-ranged electrostatic energy can be treated classically in each case. This allows us to decouple the electrostatic and the quantum (ionization) contributions (see supplementary information for the detailed derivation). The IP as computed using Equation 3 is called IP_{model} in the rest of this work. From this formula, we can identify the empirical value of δ from IP_{fit} in Equation 1 as the electrostatic dipole energy ($E_e\left([A^{-}S^{+}]\right) - E_e\left(A^{-}\right) - E_e\left(S^{+}\right)$). The fact that this value seems constant across the different chemistries is due to the fact that the electrostatic energy depends on the anion-solvent distance and their unit charges, and for all the systems reported here this distance is roughly the same considering averages across different configurations.

In order to examine the accuracy of this model, we use the same geometries for the isolated anion and solvent to compute their vertical IP (without changing the geometry). The electrostatic energies are computed for the isolated anion and solvent, for the initial and oxidized cases, as well as for the pair combinations, and from that we obtain the electrostatic contributions appearing in Equation 3. Electrostatic energies are defined and computed as the sum of the core-core interactions, the core-electron interactions and the Hartree energy for the classical electron-electron interaction (all of which are extracted from the DFT computations for the isolated species as well as pairs). We see good agreement between $\text{IP}_{\Delta\text{SCF}}$ and IP_{model} across most configurations. Thus, the description of the charge transfer effect using decoupling of the quantum and electrostatic energies of the isolated molecules and pairs seems to hold up across multiple chemistries and configurations. The most significant

deviation of the model from the ΔSCF result occurs for configurations involving PC and strong anions, (BF_4^- , PC) and (PF_6^- , PC). The only approximation in the model is the absence of coupling in quantum energy between the anion and solvent, therefore these deviations are possibly due to anion-solvent coupling, given that these anions are compact and may approach the solvent closely enough. We note, however, that analysis of charge densities confirms that only one molecule is oxidized in all cases, meaning that charge transfer is complete. Table 2 summarizes the main findings of this work, showing the average $IP_{\Delta SCF}$, the average IP_{model} as predicted from the simple charge transfer model (from Equation 3), IP_{fit} (from Equation 1), as well as the species that is oxidized. We see that these last two models predict quite well the full first-principles $IP_{\Delta SCF}$ of the anion-solvent pairs. This provides clear evidence that the anion-solvent weakening effect observed in our ΔSCF calculations originates from charge transfer and electrostatic coupling between the two species. We can also explain why the spread of the IP distribution is smaller for chemistries where the anion is oxidized than for chemistries where the solvent is oxidized. Indeed because the dipole interaction energy δ depends on the relative distance and orientation of the solvent around the anion, this energy - and therefore the IP of the pair - varies more between different configurations. Thus for two different chemistries where the average IP of the pair is roughly the same, the onset of the electrolyte degradation may happen at lower voltages if the solvent is the oxidized species, due to a wider spread of the IP values.

Finally, we further demonstrate the validity of the charge transfer model for these systems by studying a case where all oxidations lead to dipole formation, and show that in such cases, the IP increases with distance until the dipole energy is too low to energetically favor oxidation of the solvent. At this point the anion is oxidized and the charge transfer effect disappears. Increasing the distance past this point does not change the total IP (which is expected since neither the initial nor the final state involves intermolecular electrostatic interaction to first order, unlike the dipole case). This is reported in Figure 4. The leftmost point in the plot (shortest distance) corresponds to the configuration as taken from the MD

Table 2: Ionization potentials for 16 anion-solvent pairs computed with different approaches. Top lines: $IP_{\Delta SCF}$ from DFT; 2nd lines: IP_{model} from eq. 3; 3rd lines: IP_{fit} from Equation 1; 4th lines: percentage of configurations where the solvent and the anion are oxidized. Mixed scenario (oxidation of anion or solvent, depending on configuration), are observed when the anion and solvent IPs differ by roughly δ.

⇓ Solvents \ Anions ⇒	TDI^-	$TFSI^-$	BF_4^-	PF_6^-
$IP_{\Delta SCF}$ IP_{model} IP_{fit} S %, A %	5.63	7.23	8.79	9.70
DMSO 9.20	5.85 5.93 5.63 0%, 100%	6.66 6.60 6.40 100%, 0%	6.24 6.27 6.40 100%, 0%	6.41 6.37 6.40 100%, 0%
DME 10.24	5.76 5.88 5.63 0%, 100%	7.28 7.09 7.23 10%, 90%	7.20 7.16 7.44 100%, 0%	7.44 7.14 7.44 100%, 0%
PC 11.72	5.90 6.06 5.63 0%, 100%	7.52 7.26 7.23 0%, 100%	8.75 9.73 8.79 100%, 0%	9.00 10.39 8.92 100%, 0%
ACN 12.66	5.77 5.79 5.63 0%, 100%	7.38 6.78 7.23 0%, 100%	9.28 9.61 8.79 60%, 40%	9.54 9.63 9.70 94%, 6%

snapshot, without increasing the intermolecular distance. Note the two regions, one where it is energetically favorable to oxidize the solvent (left part) and the right part where it is more favorable to oxidize the anion. The increase in IP in the left part fits the following formula:

$$IP\left([A^- S^0]\right) = IP\left(S^0\right) - \delta \approx IP\left(S^0\right) - \frac{\alpha}{r} \tag{4}$$

where the second term represents the dipole energy of point charges. The coefficient α is found to be 15 eV Å, which is close to 14.4 eV Å, corresponding to the case of two point unit

charges in vacuum. The distance r considered here is taken to be the distance between the nitrogen atom of the $TFSI^-$ anion and the sulfur atom of the DMSO solvent. We verify that the IP in the right part of the plot is constant with respect to distance. Thus even a simple point charge electrostatic model accurately captures the charge-transfer transition and can therefore be used to estimate the contribution of intermolecular electrostatics to the balance between anion or solvent oxidation. We also note that the overall IP is a non-decreasing function of the separation distance, which suggests that larger molecular species may be more favorable for stability, keeping IP values constant. This consideration points to the possibility of optimizing the electrolyte's stability not only by varying the IP of the anion and the solvent but also by tuning the anion's first solvation shell radius.

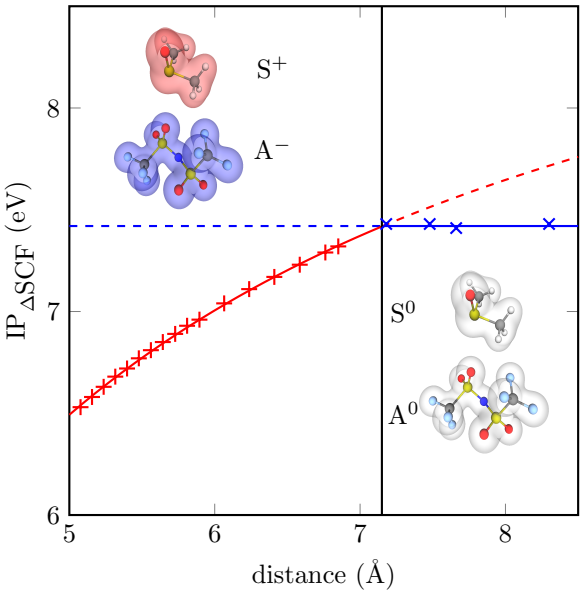

Figure 4: $IP_{\Delta SCF}$ for a ($TFSI^-$, DMSO) configuration, with respect to the increasing distance (leftmost point in the plot is the initial configuration). The red marks correspond to situations where the solvent is oxidized, the blue marks to situations where the anion is oxidized. The distance plotted here is the distance between the nitrogen atom of the $TFSI^-$ anion and the sulfur atom of the DMSO solvent. The IP for the right part of the plot (where the anion is oxidized) is constant with distance. As shown by the solid red line, the dependence of the left part of the plot is accurately captured by a fit with the formula $IP = \text{constant} - \frac{\alpha}{r}$.

Possible degradation mechanisms

Previous studies examined the possibility of hydrogen transfer after oxidation,[15,17,20] suggesting that it is the reason for the weakening of the combined solvent-anion system. We have shown that the weakening effect of the anion-solvent pair can be explained regardless of any specific degradation steps following the system oxidation. However, the study of electrostatic intermolecular interactions shown above can give new insight into the oxidation-driven reaction mechanisms. Without doing an exhaustive study of reaction mechanisms and their energy barriers, this section focuses on the impact of the proton (ionic charge) transfer mechanism. We postulate that H transfer is energetically favorable in the cases of charge-transfer complexes partly because of electrostatics, since it would compensate the dipole formation and lower the electrostatic energy. In this work, using the same configuration of anion-solvent pairs, no spontaneous intermolecular reaction was observed when we relaxed the geometries. We proceeded to study H transfer by initially displacing H towards the anion, followed by relaxation of the oxidized structure. We found that in those anion-solvent pairs where the charge-transfer dipole was formed (i.e. solvent oxidized), an H atom from the solvent was observed to transfer to the anion in about 80% of the configurations. In all cases, if the structure was not oxidized, the H atom relaxed to the initial structure. For the anion-solvent pairs where oxidation results in electronic charge transfer, hydrogen transfer indeed lowers the dipole moment and total energy of the system. In the case of BF_4^- and PF_6^- anions, the hydrogen atom transfers to a fluorine, forming HF, leaving a BF_3 or PF_5. Figure 5 shows typical snapshots of configurations with charge transfer. We conclude that hydrogen transfer is not the cause of the electrolyte weakening but rather a consequence of the intrinsic electronic charge-transfer complex formation, governed by the interplay between (quantum) ionization and (classical) electrostatic dipole energetics. An exhaustive research of degradation mechanisms and energy barriers in light of the findings of this work will be addressed in a future article.

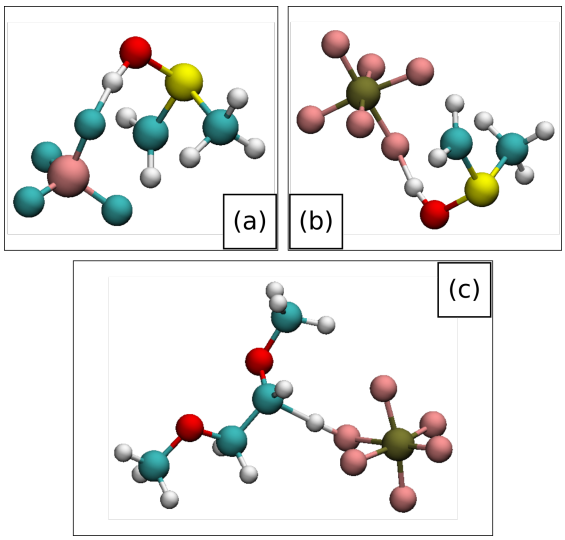

Figure 5: Hydrogen transfer for different anion-solvent pairs. Figure a) corresponds to the (BF_4^- , DMSO) pair, figure b) corresponds to the (PF_6^- , DMSO) pair and figure c) corresponds to the (PF_6^- , DME) pair.

Effects of solvation

In our above study of charge transfer complex formation we explicitly considered pairs of anion and solvent molecules in vacuum. In this section we examine the effect of solvation on the oxidation energetics and the electrostatic interaction between the electrolyte species. Our main finding is that solvation quantitatively changes the electrostatic dipole energy in the presence of solvent (denoted by $\delta_\bullet$) primarily due to the dielectric screening effect due to the solvent, and we are able to explain the trends across several solvent-salt combinations again using a simple electrostatic model derived from the above understanding of the charge-transfer complex. First we look at the dependence of the IP on the number of solvent molecules in the explicitly solvated scenario. We find that the average IP increases with the number of solvents (up to five solvent molecules, see figure S5 in supplementary information). This increasing trend is expected from classical electrostatic energy of a charge in a dielectric medium, and can be understood as a polarization effect of the additional solvents, i.e. that anion (negative species) IP increases and solvent (neutral species) IP decreases with the solvent dielectric constant. We note in passing that in order to obtain accurate IP values for

explicitly solvated systems, a proper extrapolation to large system size is needed,[57] which requires expensive simulations that lie outside the scope of our investigation. It is also important to note that in all the explicitly solvated computations there is still only one species that is fully oxidized upon removal of charge (whether it is the anion or one of the solvents). We again emphasize that for this to happen it is critical to choose an exchange correlation functional with minimal delocalization errors, such as M06-HF. Therefore, the smallest unit that is needed to study oxidation is the explicit anion-solvent pair, and addition of the full solvation affects the results only through polarization. To analyze the long-range effect of full solvation, and in particular the change in $\delta_\bullet$, we employ the PCM implicit solvent model for all the BF_4^- pairs (i.e., BF_4^- solvated with DMSO, DME, PC or ACN) with dielectric constants of 46.8 for DMSO, 4.2 for DME, 65.5 for PC, and 35.7 for ACN. We find that the solvent is still the oxidized species, just like in the vacuum case, and the value of the difference $\delta_\bullet$ between the IP of the solvent and that of the solvent-anion pair is indeed lower but still significant in the PCM-solvated calculations. The values of $\delta_\bullet$ are reported in table S7 of the supplementary information. To understand the trend, we introduce the effect of solvation into the model of Equation 3, treating it as an effect of classical dielectric continuum on the energy of point charges. The computational finding that δ decreases in solvated systems is expected, because it represents the classical electrostatic energy of the dipole formation, which should decrease with increasing dielectric constant (denoted by ϵ). The detailed derivation of the effect of full solvation in the value of the dipole stabilization energy δ is given in the supplementary information. Following the discussion the supplementary information (see equation S4), the value of the electrostatic stabilization energy at full solvation is given by $\delta_\bullet = \delta/\epsilon$. Thus the value of $\delta_\bullet$ in PCM-solvation for DME is much closer to the vacuum value of than for the other three solvents, which we expect given that DME has a much lower dielectric constant. In fact we find that the value of $\delta_\bullet$ can be approximated even without PCM calculations and only using the equation above starting with the value of δ computed in vacuum and the dielectric constant ϵ of the solvent.

Table S7 shows the comparison between this approximation and the computed value for $\delta_\bullet$. When we compare the values of $\delta_\bullet$ from PCM calculations to δ/ϵ (where the vacuum value δ is about 2.8 eV) averaged over 5 configurations chosen close to the IP distribution peak, we find that the difference ranges from 0.03 to 0.07 eV. Therefore we have a practical, fast recipe for estimating IP of the full solvent-anion system that requires only computations of IP of individual solvated species.

Conclusions

This study shows that oxidative stability of Li-ion battery electrolytes is governed by non trivial coupling between anion and solvent and requires their coupling to be simulated explicitly. We find that only one molecule, either the solvent or the anion, is oxidized upon oxidation, but the value of the ionization potential (IP) depends on the chemistry of the components. The overall oxidative stability of the combined solvent-anion system is often significantly lower than the stability of each individual species, and increasing the IP of one of them does not necessarily increase the stability of the resulting electrolyte. By computationally examining a wide range of anion and solvent combinations we find a universal coupling behavior which is explained by the formation of a charge transfer complex upon oxidation, depending on the IP of anions and solvents and their electrostatic interaction. We construct a simple model based on this understanding that is able to quantitatively capture the oxidative stability of very different electrolytes and predicts trends that are consistent with experimental observations. We emphasize that common semi-local density functionals suffer from charge delocalization errors when describing oxidation of representative molecular clusters and are likely to miss the qualitative features and the magnitude of the charge transfer effect that is determined by the electrostatic interaction between local charges resulting from ionization. Using this model, we show how the IP of the pair can be approximated in a simple way, whether in vacuum or in full solvation. We find that hydrogen abstraction

from solvent is not the primary reason for the electrolyte's weakening but is more likely to subsequently occur after a charge-transfer complex is formed upon oxidation. Thus, this is expected to be a likely common second step in the decomposition process. Results presented here provide direct implications and quantitative rules for designing stable battery electrolytes, emphasizing that both solvent and salt anions must be optimized as a whole.

Conflict of Interests

There authors declare no competing financial interests.

Author Contributions

E. R. F., G. S., F. F. and B. K. performed the quantum calculations, formulated and verified the charge transfer model. N.M. and J. P. M. performed MD calculations and extracted the structures. J. C. G., W. A. G. and B. V. M. gave technical support and conceptual advice. B. K. conceived and supervised the study.

Acknowledgements

We acknowledge useful discussions with Heather Kulik and Mordechai Kornbluth. Funding for E. R. F. was provided by Robert Bosch LLC, partly through the MIT Energy Initiative fellowship.

References

(1) Tarascon, J.-M.; Armand, M. *Nature* **2001**, *414*, 359–367.

(2) Goodenough, J. B.; Kim, Y. *Chemistry of materials* **2009**, *22*, 587–603.

(3) Nakayama, M.; Wada, S.; Kuroki, S.; Nogami, M. *Energy & Environmental Science* **2010**, *3*, 1995–2002.

(4) Kaneko, F.; Wada, S.; Nakayama, M.; Wakihara, M.; Koki, J.; Kuroki, S. *Advanced Functional Materials* **2009**, *19*, 918–925.

(5) Bhatt, M. D.; O'Dwyer, C. *Physical Chemistry Chemical Physics* **2015**, *17*, 4799–4844.

(6) Gauthier, M.; Carney, T. J.; Grimaud, A.; Giordano, L.; Pour, N.; Chang, H.-H.; Fenning, D. P.; Lux, S. F.; Paschos, O.; Bauer, C.; Maglia, F.; Lupart, S.; Lamp, P.; Shao-Horn, Y. *The Journal of Physical Chemistry Letters* **2015**, *6*, 4653–4672.

(7) Leung, K. *The Journal of Physical Chemistry C* **2012**, *117*, 1539–1547.

(8) Kazemiabnavi, S.; Dutta, P.; Banerjee, S. *The Journal of Physical Chemistry C* **2014**, *118*, 27183–27192.

(9) Zhang, X.; Pugh, J. K.; Ross, P. N. *Journal of The Electrochemical Society* **2001**, *148*, E183–E188.

(10) Husch, T.; Yilmazer, N. D.; Balducci, A.; Korth, M. *Physical Chemistry Chemical Physics* **2015**, *17*, 3394–3401.

(11) Xia, L.; Tang, B.; Yao, L.; Wang, K.; Cheris, A.; Pan, Y.; Lee, S.; Xia, Y.; Chen, G. Z.; Liu, Z. *ChemistrySelect* **2017**, *2*, 7353–7361.

(12) Korth, M. *Physical Chemistry Chemical Physics* **2014**, *16*, 7919–7926.

(13) Ong, S. P.; Andreussi, O.; Wu, Y.; Marzari, N.; Ceder, G. *Chemistry of Materials* **2011**, *23*, 2979–2986.

(14) Marenich, A. V.; Ho, J.; Coote, M. L.; Cramer, C. J.; Truhlar, D. G. *Physical Chemistry Chemical Physics* **2014**, *16*, 15068–15106.

(15) Borodin, O.; Jow, T. R. *ECS Transactions* **2011**, *33*, 77–84.

(16) Xing, L.; Borodin, O.; Smith, G. D.; Li, W. *The Journal of Physical Chemistry A* **2011**, *115*, 13896–13905.

(17) Borodin, O.; Behl, W.; Jow, T. R. *The Journal of Physical Chemistry C* **2013**, *117*, 8661–8682.

(18) Borodin, O.; Olguin, M.; Spear, C. E.; Leiter, K. W.; Knap, J. *Nanotechnology* **2015**, *26*, 354003.

(19) Delp, S. A.; Borodin, O.; Olguin, M.; Eisner, C. G.; Allen, J. L.; Jow, T. R. *Electrochimica Acta* **2016**, *209*, 498–510.

(20) Kim, D. Y.; Park, M. S.; Lim, Y.; Kang, Y.-S.; Park, J.-H.; Doo, S.-G. *Journal of Power Sources* **2015**, *288*, 393–400.

(21) Wang, Y.; Xing, L.; Borodin, O.; Huang, W.; Xu, M.; Li, X.; Li, W. *Physical Chemistry Chemical Physics* **2014**, *16*, 6560–6567.

(22) Arakawa, M.; Yamaki, J.-i. *Journal of power sources* **1995**, *54*, 250–254.

(23) Ue, M.; Murakami, A.; Nakamura, S. *Journal of The Electrochemical Society* **2002**, *149*, A1572–A1577.

(24) Ortiz, D.; Gordon, I. J.; Legand, S.; Dauvois, V.; Baltaze, J.-P.; Marignier, J.-L.; Martin, J.-F.; Belloni, J.; Mostafavi, M.; Le Caër, S. *Journal of Power Sources* **2016**, *326*, 285–295.

(25) Kanamura, K.; Umegaki, T.; Ohashi, M.; Toriyama, S.; Shiraishi, S.; Takehara, Z.-i. *Electrochimica Acta* **2001**, *47*, 433–439.

(26) Moshkovich, M.; Cojocaru, M.; Gottlieb, H.; Aurbach, D. *Journal of Electroanalytical Chemistry* **2001**, *497*, 84–96.

(27) Perdew, J. P.; Burke, K.; Ernzerhof, M. *Physical review letters* **1996**, *77*, 3865.

(28) Becke, A. D. *The Journal of chemical physics* **1993**, *98*, 5648–5652.

(29) Cohen, A. J.; Mori-Sánchez, P.; Yang, W. *Science* **2008**, *321*, 792–794.

(30) Lage-Estebanez, I.; Ruzanov, A.; de la Vega, J. M. G.; Fedorov, M. V.; Ivaništšev, V. B. *Physical Chemistry Chemical Physics* **2016**, *18*, 2175–2182.

(31) Zhao, Y.; Truhlar, D. G. *Theoretical Chemistry Accounts: Theory, Computation, and Modeling (Theoretica Chimica Acta)* **2008**, *120*, 215–241.

(32) Zhao, Y.; Truhlar, D. G. *The Journal of Physical Chemistry A* **2006**, *110*, 5121–5129.

(33) Zhao, Y.; Truhlar, D. G. *The Journal of Physical Chemistry A* **2006**, *110*, 13126–13130.

(34) Ghosh, D.; Roy, A.; Seidel, R.; Winter, B.; Bradforth, S.; Krylov, A. I. *The Journal of Physical Chemistry B* **2012**, *116*, 7269–7280.

(35) Parson, W. W.; Creighton, S.; Warshel, A. *Journal of the American Chemical Society* **1989**, *111*, 4277–4284.

(36) Barnes, T. A.; Kaminski, J. W.; Borodin, O.; Miller III, T. F. *The Journal of Physical Chemistry C* **2015**, *119*, 3865–3880.

(37) Qu, X.; Jain, A.; Rajput, N. N.; Cheng, L.; Zhang, Y.; Ong, S. P.; Brafman, M.; Maginn, E.; Curtiss, L. A.; Persson, K. A. *Computational Materials Science* **2015**, *103*, 56–67.

(38) Mulliken, R. S. *The Journal of Chemical Physics* **1955**, *23*, 1833–1840.

(39) Frisch, M. J.; al., Gaussian 03, Revision C.02. Gaussian, Inc., Wallingford, CT, 2004.

(40) Krishnan, R.; Binkley, J. S.; Seeger, R.; Pople, J. A. *The Journal of Chemical Physics* **1980**, *72*, 650–654.

(41) McLean, A.; Chandler, G. *The Journal of Chemical Physics* **1980**, *72*, 5639–5648.

(42) Molinari, N.; Khawaja, M.; Sutton, A.; Mostofi, A. *The Journal of Physical Chemistry B* **2016**, *120*, 12700–12707.

(43) Molinari, N.; Mailoa, J. P.; Kozinsky, B. *Chemistry of Materials* **2018**, *30*, 6298–6306.

(44) Hoover, W. G. *Physical review A* **1985**, *31*, 1695.

(45) Nosé, S. *The Journal of chemical physics* **1984**, *81*, 511–519.

(46) Hoover, W. G. *Physical Review A* **1986**, *34*, 2499.

(47) Plimpton, S.; Crozier, P.; Thompson, A. *Sandia National Laboratories* **2007**, *18*.

(48) Banks, J. L. et al. *Journal of Computational Chemistry* **2005**, *26*, 1752–1780.

(49) Valiev, M.; Bylaska, E.; Govind, N.; Kowalski, K.; Straatsma, T.; Dam, H. V.; Wang, D.; Nieplocha, J.; Apra, E.; Windus, T.; de Jong, W. *Computer Physics Communications* **2010**, *181*, 1477 – 1489.

(50) Kendall, R. A.; Dunning Jr, T. H.; Harrison, R. J. *The Journal of chemical physics* **1992**, *96*, 6796–6806.

(51) Neese, F. *Wiley Interdisciplinary Reviews: Computational Molecular Science* **2012**, *2*, 73–78.

(52) Becke, A. D. *Physical review A* **1988**, *38*, 3098.

(53) Iikura, H.; Tsuneda, T.; Yanai, T.; Hirao, K. *The Journal of Chemical Physics* **2001**, *115*, 3540–3544.

(54) Ue, M.; Takeda, M.; Takehara, M.; Mori, S. *Journal of The Electrochemical Society* **1997**, *144*, 2684–2688.

(55) Xu, K. *Chemical reviews* **2004**, *104*, 4303–4418.

(56) Xing, L.; Borodin, O. *Physical Chemistry Chemical Physics* **2012**, *14*, 12838–12843.

(57) Tazhigulov, R. N.; Bravaya, K. B. *J. Phys. Chem. Lett* **2016**, *7*, 2490–2495.